

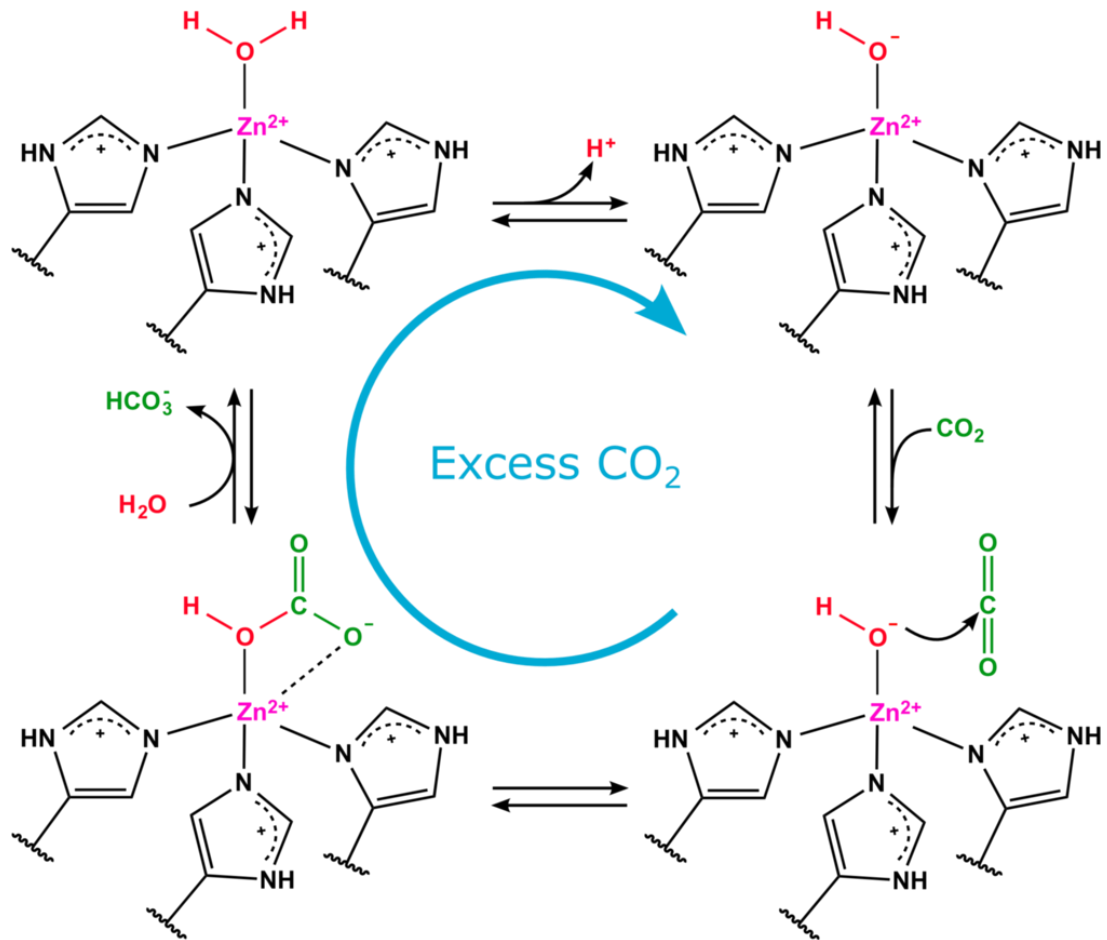
# Supplementary Information

## Ultra-thin nano-stabilized enzymatic liquid membrane for CO<sub>2</sub> separation and capture

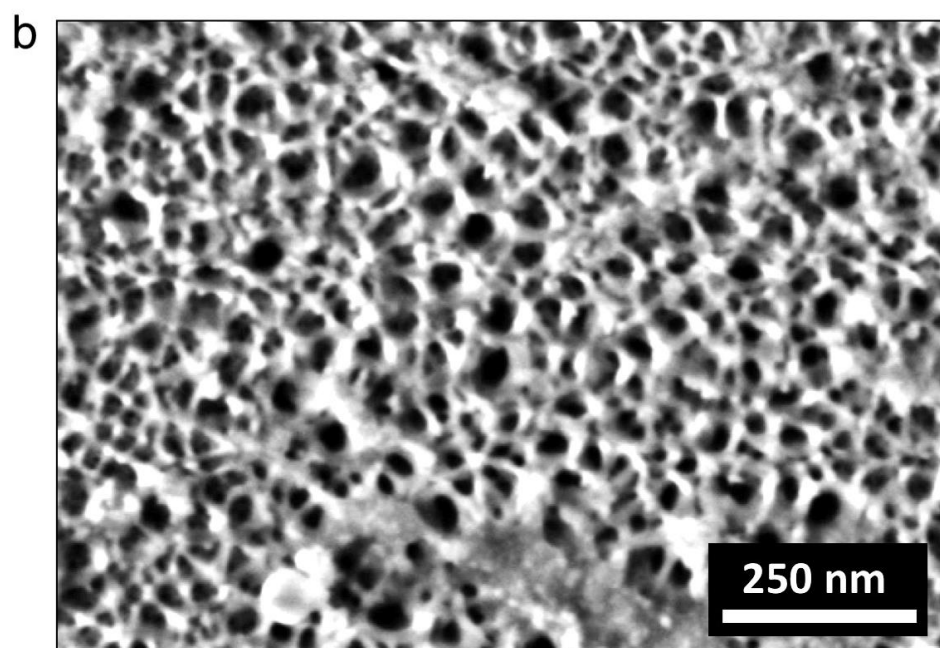
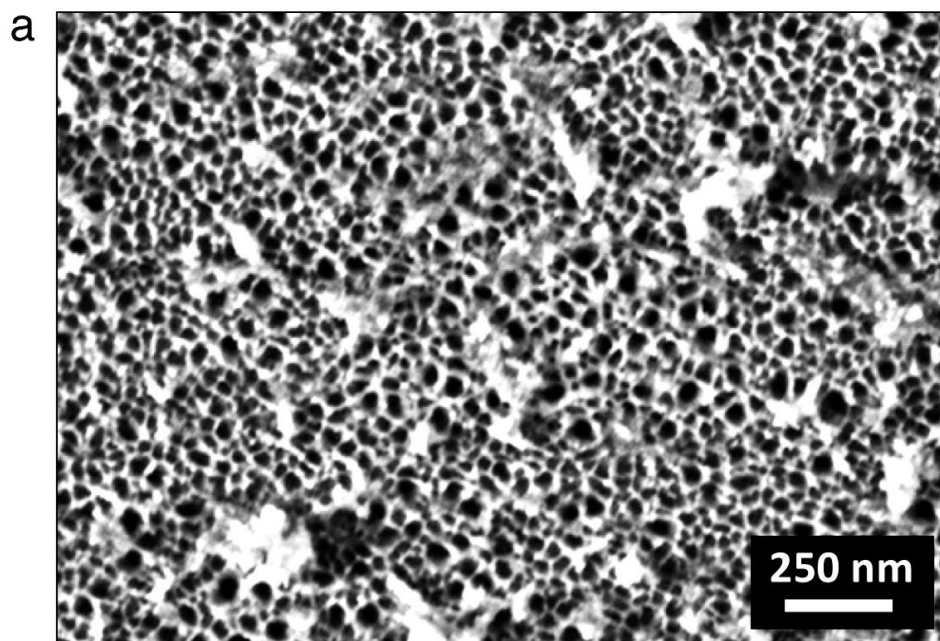
Yaqin Fu<sup>1,2</sup>, Ying-Bing Jiang<sup>\*,1,2,3</sup>, Darren Dunphy<sup>1,2</sup>, Haifeng Xiong<sup>1,2</sup>, Eric Coker<sup>4</sup>, Stan Chou<sup>4</sup>, Hongxia Zhang<sup>5</sup>, Juan M. Vanegas<sup>4</sup>, Jonas G. Croissant<sup>1,2</sup>, Joseph L. Cecchi<sup>1</sup>, Susan B Rempe<sup>4</sup> & C. Jeffrey Brinker<sup>\*,1,2,4</sup>

### TABLE OF CONTENT

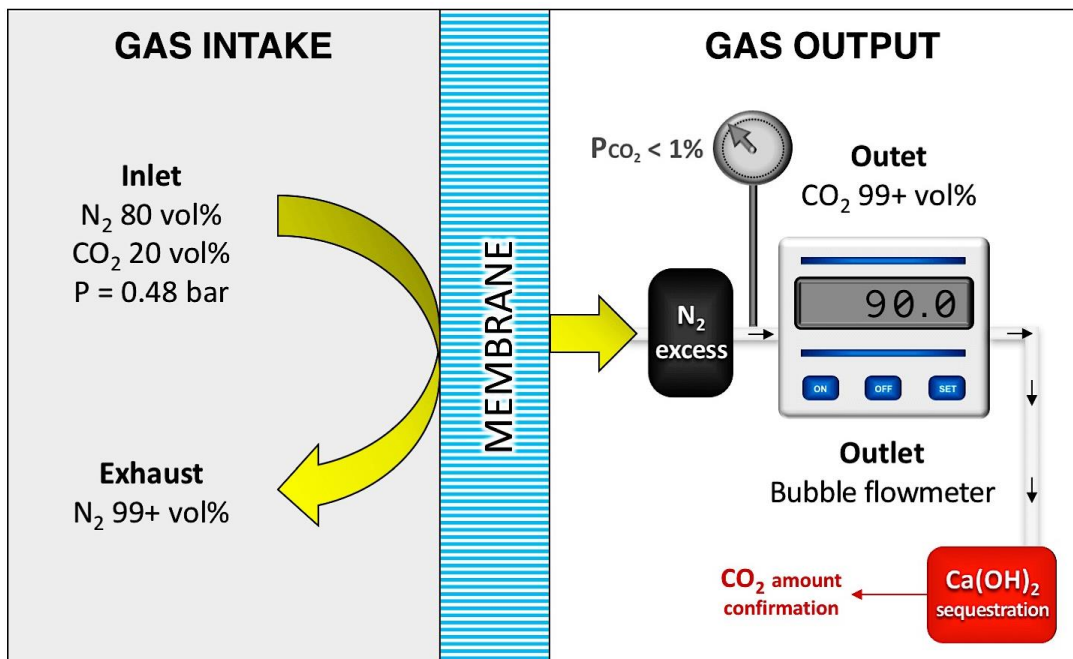
<b>Supplementary Figure 1   Enzymatic active site structure during the catalytic cycle.....</b>	<b>p. 2</b>
<b>Supplementary Figure 2   Microscopy images of the Anodisc support.....</b>	<b>p. 3</b>
<b>Supplementary Figure 3   CO<sub>2</sub>/N<sub>2</sub> separation set-up.....</b>	<b>p. 4</b>
<b>Supplementary Figure 4   CO<sub>2</sub>/N<sub>2</sub> gas chromatography analysis.....</b>	<b>p. 5</b>
<b>Supplementary Figure 5   CO<sub>2</sub>/H<sub>2</sub> separation set-up.....</b>	<b>p. 6</b>
<b>Supplementary Figure 6   Selectivity of the CO<sub>2</sub>/H<sub>2</sub> separation as a function of time.....</b>	<b>p. 7</b>
<b>Supplementary Figure 7   Stability of the enzymatic liquid membrane overtime.....</b>	<b>p. 8</b>
<b>Supplementary Discussion.....</b>	<b>p. 9</b>
<b>Supplementary Discussion.....</b>	<b>p. 10</b>
<b>Supplementary Discussion.....</b>	<b>p. 11</b>



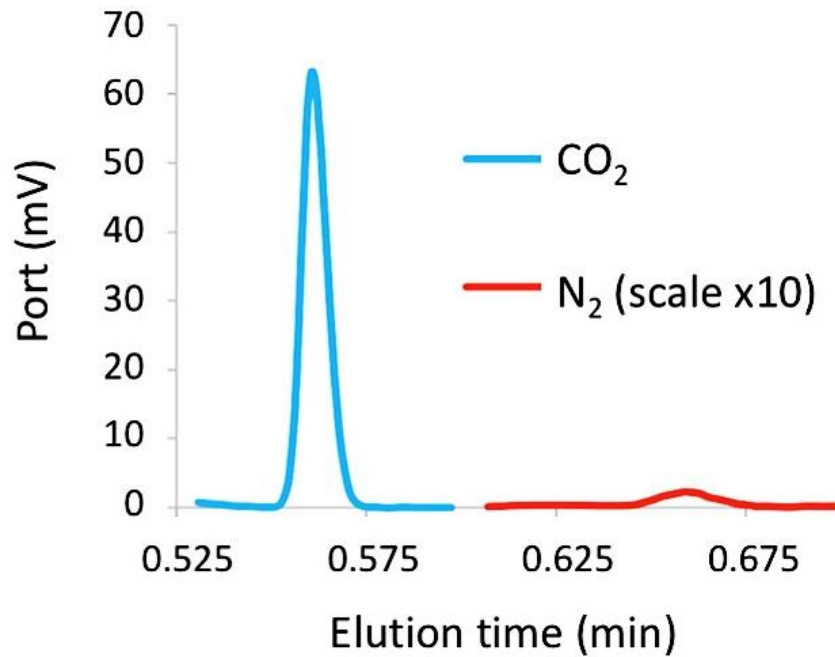
**Supplementary Figure 1 | Enzymatic active structure site during the catalytic cycle.** Key reactions catalyzed by carbonic anhydrase enzyme, viewed from the active site. A zinc ion ( $Zn^{2+}$ ) coordinated with three histidine residues greatly enhances the acidity of the zinc-bound water molecule. A chain of protonatable residues shuttles the water proton out of the active site to avoid back-reaction. The active site orients  $CO_2$  near the deprotonated water ( $OH^-$ ). As a result, the enzyme dramatically accelerates  $CO_2$  hydration to bicarbonate ion ( $HCO_3^-$ ), even when the solution is neutral.



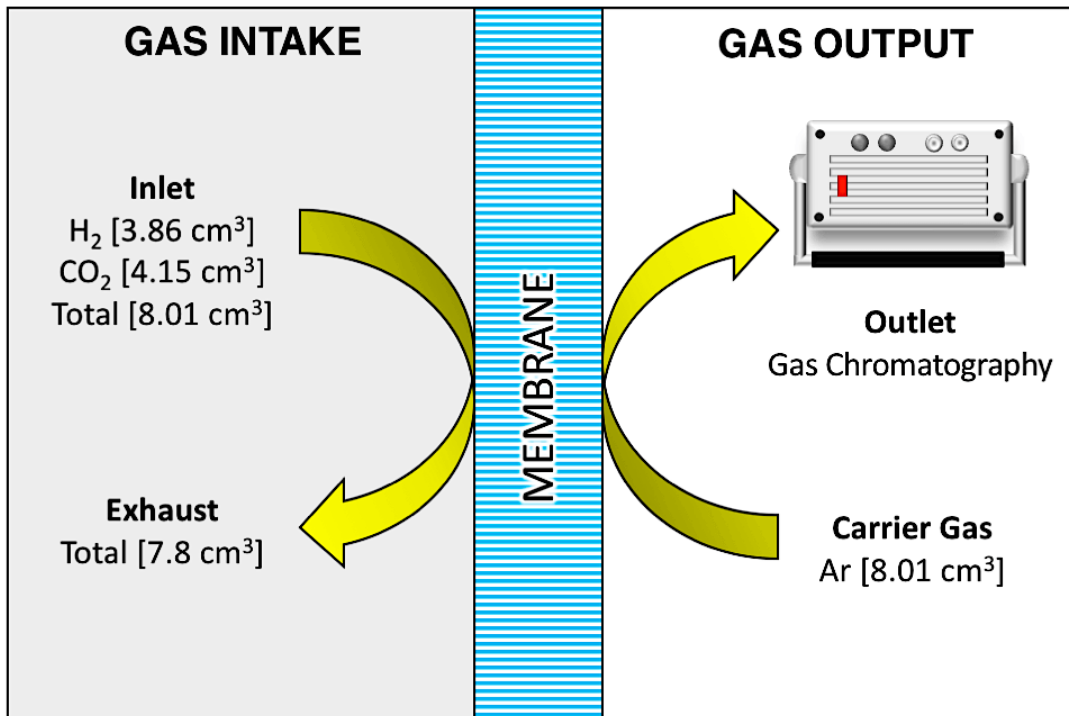
**Supplementary Figure 2 | Microscopy images of the Anodisc support.** (a-b) Plan-view SEM images of the Anodisc at two magnification scales showing the size distribution of the Anodisc mesopores, which constitute ca 70% of the Anodisc surface.



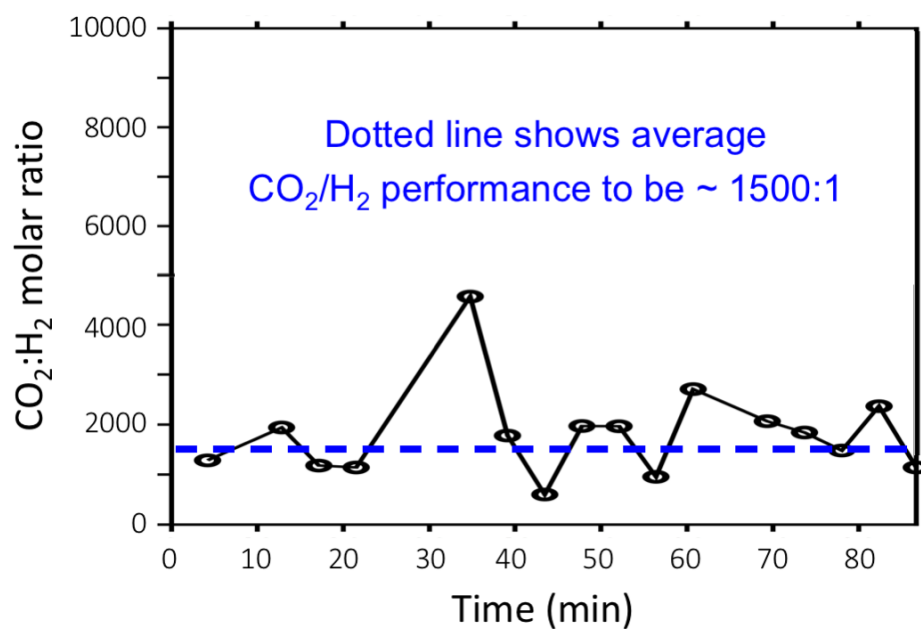
**Supplementary Figure 3 | CO<sub>2</sub>/N<sub>2</sub> separation set-up.** On the gas intake side, the feed gas composition was 20 vol% CO<sub>2</sub> in N<sub>2</sub> maintained at an ambient pressure in order to simulate the major composition of flue gas from a coal-fired plant. On the gas output side, a bubble flow rate meter was used to measure the flow rate, and the CO<sub>2</sub> pressure was maintained at ambient atmospheric pressure. An excess amount of pure N<sub>2</sub> was pre-stored in order to keep the CO<sub>2</sub> partial pressure below 1% during the bubble flowmeter measurement. A Ca(OH)<sub>2</sub> solution was used to collect and determine the permeated CO<sub>2</sub> content and maintain a constant chemical potential driving force for CO<sub>2</sub> separation.



**Supplementary Figure 4 | CO<sub>2</sub>/N<sub>2</sub> gas chromatography analysis.** Gas chromatograph showing composition of the output gas through the enzymatic liquid membrane, plotted as signal strength as a function of time, when the input feed is a 1:1 mixture of CO<sub>2</sub> and N<sub>2</sub> gas. Here, the CO<sub>2</sub> to N<sub>2</sub> selectivity is above 750.

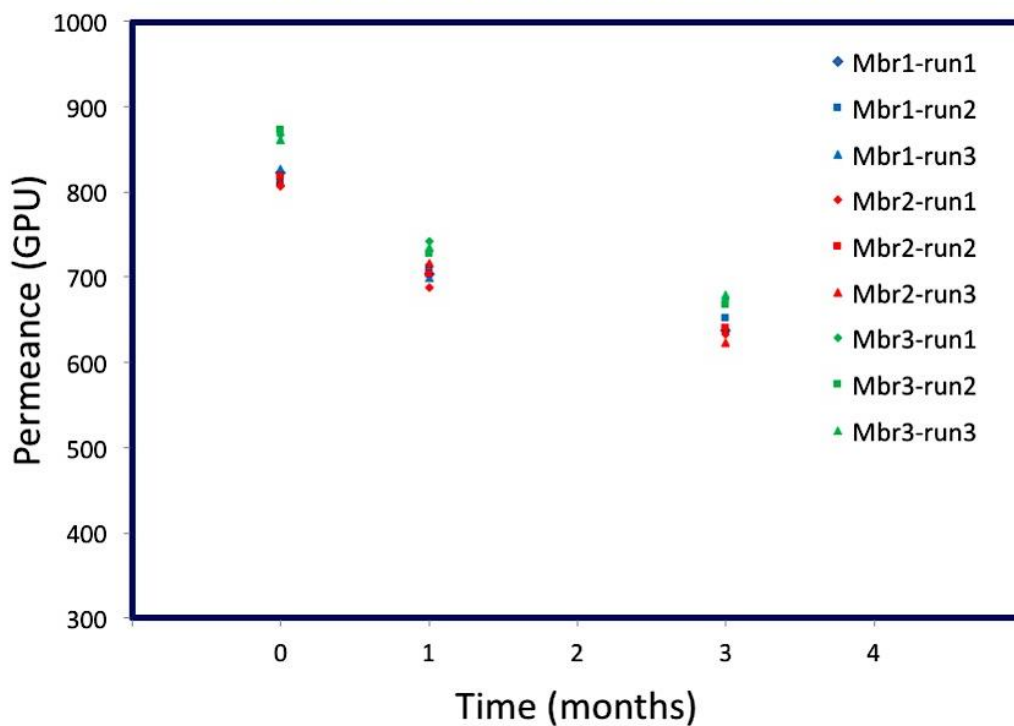


**Supplementary Figure 5 | CO<sub>2</sub>/H<sub>2</sub> separation set-up.** A cross flow configuration was used for H<sub>2</sub> permeation measurements. Feed gas composition was fixed at 43% H<sub>2</sub> and 57% CO<sub>2</sub>. The quantity of gas permeating across the membrane was calculated by the difference in gas flow at the inlet versus the exhaust, with a typical cross-flow rate of 0.21 cm<sup>3</sup>. Gas permeated across the membrane was then carried by an Ar gas (8.01 cm<sup>3</sup>) into a calibrated Inficon 3000 Micro GC gas analyzer for quantitative measurement discrimination.



**Supplementary Figure 6 | Selectivity of the CO<sub>2</sub>/H<sub>2</sub> separation as a function of time.** Each data point was acquired via a gas chromatography run.

### MEMBRANE PERFORMANCE STABILITY



**Supplementary Figure 7 | Stability of the enzymatic liquid membrane overtime maintained at >90%RH.** The CO<sub>2</sub> permeance of the enzymatic liquid membranes (N=3) shows a moderate and limiting loss of permeance over 3 months, but the permeance exceeds that of most polymeric membranes and the CO<sub>2</sub>/N<sub>2</sub> selectivity remains above 500.



## SUPPLEMENTARY DISCUSSION

### ❖ DETERMINATION OF THE RELATIVE HUMIDITY NECESSARY FOR THE STABILITY OF MEMBRANES WITH VARIOUS PORE SIZES

$$\ln \frac{P_v}{P_{\text{sat}}} = - \frac{2H \gamma V_m}{RT}$$

$P_v$  : equilibrium vapor pressure

$P_{\text{sat}}$  : saturation vapor pressure

RH : relative humidity

$$\ln(\text{RH}) = - \frac{2 \gamma V_m}{r RT}$$

H : average meniscus curvature

$\gamma$  : liquid-air surface tension

$$= - \frac{2 \times 0.072 (\text{N m}^{-1}) \times 18 (\text{cm}^3 \text{mol}^{-1})}{r \times 8.32 (\text{J mol}^{-1} \text{K}^{-1}) \times 298 (\text{K})}$$

$V_m$  : liquid molar volume

R : ideal gas constant

$r = 3 \text{ nm}$  (6 nm pores); RH = 65.2 %

T : temperature

$r = 4 \text{ nm}$  (8 nm pores); RH = 73.9 %

r : radius of the membrane

### ❖ CONCLUSION

Will the membrane dry out under the operation conditions? No, 6 to 8 nm-wide highly hydrophilic pores capture and hold water at about 70% humidity. A typical flue gas comprises 6.2 wt% H<sub>2</sub>O if it is from a coal-fired plant, and 14.6 wt% H<sub>2</sub>O if it is from a gas-fired plant. Both are much higher than the saturated water vapor concentration at 40 °C (~50g H<sub>2</sub>O /kg air or 0.5 wt% H<sub>2</sub>O).

## SUPPLEMENTARY DISCUSSION

### ❖ **NANOPORE CAPILLARY PRESSURE EQUATION FOR WATER CONDENSED IN A HYDROPHILIC PORE WITH LIQUID CONTACT ANGLE 0**

$$P = \frac{2 \gamma \cdot \cos \theta}{d} = \frac{0.144 \text{ (Pa)}}{d \text{ (m)}} \\ = \frac{1.42 \text{ (atm)}}{d \text{ (\mu m)}} \\ = \frac{2.8 \text{ (atm)}}{d \text{ (\mu m)}}$$

P : pressure on the membrane

d : diameter of the membrane

$\gamma$  : liquid-air surface tension

$\theta$  : liquid contact angle

d = 1  $\mu\text{m}$  (1  $\mu\text{m}$  pores); P = 2.8 atm

d = 10 nm (10 nm pores); P = 28 atm

d = 8 nm (8 nm pores); P = 35 atm

### ❖ **CONCLUSION**

Will the membrane be stable under higher pressures? Yes, because of the capillary pressure, the enzymatic liquid membrane can withstand tens of atmospheres of pressure and should not be displaced from the membrane under operation.

## SUPPLEMENTARY DISCUSSION

### ❖ DETERMINATION OF THE AREAL DENSITY OF 8 nm SILICA MESOPORES EXPOSED ON THE ANODISC SUPPORT SURFACE

**Step 1:** Determine the areal density of mesopores in individual Anodisc pores by image analysis.

Procedure: direct TEM imaging of mesopore arrays within Anodisc pores and determination of the numbers of mesopores per  $\text{cm}^2$ .

Result:  $5.60 \times 10^{11}$  nanopores per  $\text{cm}^2$ .

**Step 2:** Determine of areal fraction of pores in Anodisc membrane support.

Procedure: direct SEM imaging of Anodisc surface (Supplementary Fig. S3) and determination of fraction porosity by random line cut analysis.

Result: 70%.

**Step 3:** Assuming that all Anodisc pores are completely filled with silica mesopores with a density of  $5.60 \times 10^{11}$  nanopores per  $\text{cm}^2$ , we calculated the areal density of silica mesopores exposed on the Anodisc surface.

Result:  $0.7 \times 5.60 \times 10^{11} = 3.92 \times 10^{11}$  nanopores per  $\text{cm}^2$ .

### ❖ CONCLUSION

The overall areal density of the alumina Anodisc support-nanoporous silica is of  $3.92 \times 10^{11}$  nanopores per  $\text{cm}^2$ .